



# 1 Aqueous particle generation with a 3D printed nebulizer

2 Michael Rösch<sup>1,2</sup>, and Daniel J. Cziczo<sup>1,3,4</sup>

3 <sup>1</sup>Department of Earth, Atmospheric & Planetary Sciences, Massachusetts Institute of Technology,  
4 Cambridge, 02139, USA

5 <sup>2</sup>Department of Environmental Systems Science, Eidgenössische Technische Hochschule - ETH, Zurich,  
6 8092, Switzerland

7 <sup>3</sup>Department of Civil Environmental Engineering, Massachusetts Institute of Technology, Cambridge,  
8 02139, USA

9 <sup>4</sup>Department of Earth, Atmospheric and Planetary Sciences, Purdue University, West Lafayette, IN 47907  
10 USA

11

12 *Correspondence to:* Michael Roesch (michael.roesch@env.ethz.ch)

13 **Abstract.** In this study, we describe the design and testing of a high output stability constant liquid feed  
14 nebulizer using the Venturi principle to generate liquid particles from solutions. This atomizer, the  
15 PRinted drOpleT Generator (PROTeGE) was manufactured using stereolithography (SLA) printing.  
16 Different concentrations of ammonium sulfate solutions were used to characterize the size and number  
17 concentration of the generated particles. A comparison of a 3D printed 0.5 mm orifice with a more  
18 dimensionally accurate and symmetric machined 0.5 mm brass orifice using the same ammonium sulfate  
19 solutions was also performed. PROTeGE is also shown to be capable of dispersing polystyrene latex  
20 spheres (PSLs) for calibration purposes. The particle number concentrations obtained in this study ranged  
21 from  $\sim 10000 \text{ cm}^{-3}$  for  $0.75 \text{ }\mu\text{m}$  to  $\sim 100 \text{ cm}^{-3}$  for  $5.0 \text{ }\mu\text{m}$  PSL particles with a dependence on the  
22 concentration of the dispersed solution. PROTeGE is easy to manufacture and operate, low in  
23 maintenance, and cost-effective for laboratory and field generation of particles from aqueous media.  
24

## 25 1 Introduction

26



27           Reliable and cost-effective particle generation methods are necessary for applications where a  
28 well-defined mono- or polydisperse particle concentrations and size is required. High concentrations of  
29 monodisperse aerosol particles ( $>10^6$  particles/cm<sup>3</sup>) in the nm to  $\mu\text{m}$  diameter size range can be created  
30 by instruments utilizing vapor condensation and electrospray techniques. Similar concentrations and size  
31 ranges of aerosol particles can be produced from bulk solutions using a variety of instruments such as  
32 vibrating-orifice aerosol generators and ultrasonic nebulizers. Another common technique used to  
33 generate liquid aerosol particles is by pressurized-air nebulization. In this method, compressed air is  
34 utilized to shatter a solution into small aerosol droplets with a specific size distribution (Swiderska-  
35 Kowalczyk et al., 1997).

36           Pressurized-air nebulizers have been used in numerous studies which require the  
37 generation of aqueous aerosol particles. For example, Wang et al. (2019) used a nebulizer to create  
38 ammonium sulfate seed particles in cloud droplet activation studies. Kong et al. (2018) created aqueous  
39 aerosol particles used to study deliquescence and ice nucleation in sea salt particles. These are two of  
40 many studies focused on the influence of aerosol particles in the Earth's atmosphere. Pressurized-air  
41 nebulizers are also used in pharmaceutical applications to produce nanometer-sized drug particles with a  
42 specific size distribution (Eerikainen et al., 2003). It is clear that the pressurized-air nebulizer is a  
43 ubiquitous instrument for studies or applications requiring aqueous aerosol particle generation. Although  
44 effective, commercial particle generation instruments may not be economically feasible for all research  
45 and teaching institutions wishing to perform these types of experiments.

46           Advances in 3D printing have made it possible to rapidly fabricate high-resolution ( $\mu\text{m}$ -scale)  
47 devices. Stereolithography (SLA), a form of 3D printing technology, creates objects in layers through the  
48 use of photopolymerization. In conjunction with Computer Aided Design (CAD), or Computer Aided  
49 Manufacturing (CAM) software, an ultraviolet (UV) laser is used to trace a pre-programmed design on  
50 to the surface of a photopolymer contained in a vat. The resin is photochemically solidified and forms a  
51 single layer of the desired object. The Form 2 SLA 3D printer (Formlabs, Inc.), used in this work, is  
52 capable of creating objects with a layer thickness of 25  $\mu\text{m}$ .

53           The Form 2 was previously used to fabricate PRIZE, a compact fluidized bed aerosol generator  
54 (Roesch et al. 2017). It was found that PRIZE was able to successfully disperse aerosol particles from dry



55 material without creating artifact particles (particles generated from the material used to fabricate the  
56 generator). The impetus for this study, similar to the study presented in Roesch et al. 2017, was to fabricate  
57 a low-cost, constant pressure nebulizer, using a SLA 3D printer, PROTeGE.

## 58 **2 Methods**

### 59 **2.1. Design**

60 PROTeGE was designed using a computer aided design (CAD) program (Solidworks 2015, Dassault  
61 Systems). There are two versions: the first is printed as a single part including a 0.5 mm diameter orifice  
62 (Fig. 1), while the second, featuring the same inner and outer dimensions, has an exchangeable nozzle to  
63 use various machined orifice diameters. The orifice used in this study is within a commercially available  
64 brass nozzle (Part Number 6183T63, McMaster-Carr) that is screwed into the pressurized air inlet of  
65 PROTeGE (Fig. 1d). This modular feature enables rapid exchange of nozzles with a different orifice  
66 diameter using the same printed unit. In contrast, the exclusively printed version of PROTeGE has a fixed  
67 orifice diameter for continuous and simple operation. Both versions are based on the generator designs of  
68 May, 1973 and Liu & Lee, 1975. Both versions include a printed GL45 bottle cap so that the aqueous  
69 material bottle can to directly attached to the nebulizer body. Unlike the repurposing of existing nebulizers  
70 built for other uses, such as medical applications (Reisner et al., 2001), PROTeGE was designed  
71 specifically for research applications e.g. instrument calibration and particle generation, similar to other  
72 custom-built nebulizers (Wex et al., 2015). In contrast to other generation systems, which are typically  
73 machined, PROTeGE is made from photopolymer resin (e.g. FLGPCL02, Formlabs Inc.), weights only  
74 ~50 g, and can therefore feature smaller overall dimensions.

75 The front inlet to PROTeGE is a 6.35 mm (0.25 in) barbed tube to connect to a pressurized airflow. The  
76 inlet is end-capped by the orifice. Directly following, and perpendicular oriented to the orifice, is the  
77 liquid feed 3.18 mm (0.125 in) inlet to the dispersible solution. Excess liquid from the nebulizing process  
78 exit the chamber through a 6.35 mm outlet at the bottom, dripping directly back into the feed bottle.  
79 Aqueous particles exit the chamber through the 9.53 mm (0.375 in) aerosol outlet at the top. The overall  
80 dimensions of PROTeGE are 17 x 45 x 65 mm (width, depth, height). Designed CAD files were converted  
81 to style files (.stl) to be readable by the 3D printer software (PreForm, Formlabs Inc.).



82

## 83 **2.2. Manufacturing**

84 The manufacturing and post-processing of the parts was performed as described by Roesch et al., 2017  
85 using the same 3D printer software, clear photopolymer resin (FLGPCL02, Formlabs Inc.) and 3D SLA  
86 printer (Form 2, Formlabs Inc.). Modifications were made to the dimensions of the default contact points  
87 of the printing scaffolding; in this study scaffolding was reduced to 0.45 mm due to the overall smaller  
88 geometry of PROTeGE (i.e., lower mass needing to be supported). Using a resolution of 100  $\mu\text{m}$ , eight  
89 complete PROTeGEs can be printed on the build surface at the same time, taking  $\sim 8$  h.

90 A custom UV box was used to post-cure the printed parts. Inside the box, the printed parts were placed  
91 on a slow moving turntable to be illuminated equally from all sides by 28 high-power LEDs emitting at  
92 405 nm. It should be noted that the curing time depends on the size and wall thickness of the printed part;  
93 one hour per mm wall thickness is suggested. The post-curing time for PROTeGE was  $\sim 1$  h. For more  
94 detailed information see the manufacturing section in Roesch et al., 2017.

95

## 96 **2.3. Experimental setup**

97 A schematic of the experimental setup including the relevant flow rates used in this study is shown in Fig.  
98 2. Dry, filtered, pressurized air was used as the carrier gas. The input flow rate of  $1.7 \text{ L min}^{-1}$  (at 35 psi)  
99 into PROTeGE was controlled by a rotameter (MR3A, Omega Engineering). A high velocity jet is created  
100 by the expansion of the pressurized air through the orifice. As a result, the pressure behind the orifice  
101 drops, the liquid is pulled upward from the feed bottle, and the high velocity jet disperses the liquid  
102 solution into droplets. Large droplets that are unable to follow the streamlines through the aerosol outlet  
103 are removed by impaction at the curved wall; these drip back as excess liquid into the feed bottle through  
104 a drain outlet at the bottom of PROTeGE. For these experiments, the droplets from the aerosol outlet were  
105 subsequently dried using a silica gel drier. Downstream, the flow of residuals (remaining solid cores of  
106 the droplets) was split into two flows. The first is sent to an optical particle sizer (OPS, Model 3330, TSI  
107 Inc.) to determine particle number size distributions (PNSD) in the size range of 0.3 to  $10 \mu\text{m}$  and the  
108 remainder through a filter (IDN-4G, Parker) open to lab. Unless otherwise noted, all experiments



109 presented here were performed using the brass nozzle with a 0.3 mm orifice and the previously stated  
110 pressures and flow rates.

111

### 112 **3. Results**

113 In this study three types of experiments were conducted to demonstrate the performance of PROTeGE:  
114 (1) An aerosol production experiment using four different sizes of polystyrene latex spheres (PSL's,  
115 Polysciences Inc., NIST traceable) ranging from 0.75 to 5.0  $\mu\text{m}$ . (2) An application experiment where  
116 different concentrated ammonium sulfate solutions were dispersed and monitored over time. (3) An  
117 experiment comparing the performance of a printed 0.5 mm orifice to a 0.5 mm brass orifice using an  
118 ammonium sulfate solution. For all experiments the PNSD of the droplet residuals (i.e., after drying) was  
119 measured with the OPS.

120 Prior to each experiment, PROTeGE was immersed in a jar with double distilled deionized (DDI) 18.2  
121  $\text{M}\Omega\cdot\text{cm}$  Millipore water and sonicated for 10 minutes in an ultrasonic bath to ensure clean inner surfaces.  
122 Afterwards, PROTeGE was dried using pressurized nitrogen and connected to the setup. Each of the four  
123 samples was prepared in a separate 100 ml glass bottle, using 80 ml of DDI water plus multiple drops of  
124 the respective PSL solution (0.75  $\mu\text{m}$ , 1.5  $\mu\text{m}$ , 2.0  $\mu\text{m}$ , 5.0  $\mu\text{m}$ ). The generated number concentration of  
125 PSL particles strongly depends on the concentration of the prepared PSL sample. Therefore, the higher  
126 the concentration of the solution, the higher the generated particle number concentration. A time-series  
127 measurement was performed for each of the four PSL samples. The obtained PNSD showed particle  
128 number concentrations from  $\sim 10000 \text{ cm}^{-3}$  for 0.75  $\mu\text{m}$  PSL particles to  $\sim 100 \text{ cm}^{-3}$  for 5.0  $\mu\text{m}$  PSL particles  
129 (Fig. 3). All four investigated PSL samples showed narrow PNSD's except the 5.0  $\mu\text{m}$  PSL sample where  
130 a fraction of sub-micrometer particles was detected (Fig. 3d). This fraction of particles likely originates  
131 from the solution matrix the PSLs are suspended in. These data show that the curved design of the  
132 chamber makes PROTeGE capable of dispersing PSL particles with diameter up to at least 5.0  
133 micrometers.

134 In addition to the PSL measurements, ammonium sulfate experiments with different solution  
135 concentrations (0.1  $\text{g L}^{-1}$ , 0.6  $\text{g L}^{-1}$ , 5.0  $\text{g L}^{-1}$ ) and an experiment to determine the performance of the  
136 printed 0.5 mm orifice versus the 0.5 mm brass orifice using the same ammonium sulfate solution of 0.6



137 g L<sup>-1</sup> were conducted. The three solutions were again prepared in separate 100 ml glass bottles using DDI  
138 water. The cleaning procedure of PROTeGE was identical to the one described above for the PSL  
139 experiments.

140 For the lowest concentration of aqueous ammonium sulfate solution (0.1 g L<sup>-1</sup>) the maximum particle  
141 number concentration of ~14000 cm<sup>-3</sup> was observed in the 0.3 μm bin of the OPS (Fig. 4a). The overall  
142 width of the generated PNSDs ranged from 0.3 μm up to 0.6 μm. Compared to the higher concentrated  
143 solutions of 0.6 g L<sup>-1</sup> and 5.0 g L<sup>-1</sup> this is rather narrow. Dispersing the 0.6 g L<sup>-1</sup> solution of ammonium  
144 sulfate generated PNSDs in the range of 0.3 μm up to 1.5 μm with a maximum particle number  
145 concentration of ~8200 cm<sup>-3</sup> in the 0.5 μm detection bin (Fig. 4b). For the highest concentration of 5.0 g  
146 L<sup>-1</sup> the generated PNSDs ranged from 1.0 μm to 2.4 μm with a maximum particle number concentration  
147 of ~7600 cm<sup>-3</sup> (Fig. 4c).

148 Overall the generated particle number concentrations for the different tested ammonium sulfate solutions  
149 will be sufficient enough to operate particle size selection instruments downstream of PROTeGE, e.g. a  
150 differential mobility analyzer (DMA), assuming ~10% of the introduced particles are selected as  
151 monodisperse aerosol particles.

152 In order to investigate the performance of an integrally printed 0.5 mm orifice versus the commercial  
153 brass nozzle the same 0.6 g L<sup>-1</sup> ammonium sulfate solution was used. Visual observations of the printed  
154 0.5 mm orifice showed that there were sometimes imperfections and asymmetries in the roundness of the  
155 printed orifice. It was therefore necessary to post-drill the printed orifice with a 0.5 mm bit by hand, and  
156 this was done for the PROTeGE used in experiments described here. The generated mean particle number  
157 concentration with the printed orifice was ~4500 cm<sup>-3</sup> versus ~2400 cm<sup>-3</sup> for the brass nozzle. Both orifices  
158 generated similar PNSDs with their maximum particle number concentrations at 0.3 μm leveling out to  
159 1.0 μm at largest (Fig. 5).

#### 160 **4. Conclusion**

161 In this study, we described the design and the performance of a low-cost particle generator – PROTeGE.  
162 The experiments presented here show the PROTeGE capability for generating four different sizes of PSL  
163 particles between 0.75 and 5.0 μm with resulting particle number concentrations between 100 cm<sup>-3</sup> and



164 ~10000 cm<sup>-3</sup>. This enables PROTeGE to be used as a simple and cost effective particle generation unit  
165 for calibration purposes. In addition, we show the results of experiments using different concentrations  
166 of ammonium sulfate solutions. The generated PNSDs ranged from 0.3 μm up to 2.4 μm with stable  
167 output concentrations demonstrating that particle size selection instruments can be used downstream of  
168 PROTeGE. Finally, we compared the performance of a commercially machined brass 0.5 mm orifice to  
169 a 3D printed 0.5 mm orifice. Both orifices performed well, while the mean particle number concentration  
170 generated with the printed orifice was almost two times higher than the particle number concentration  
171 generated with the brass orifice. Due to the low cost of PROTeGE multiple generators can be used in  
172 parallel to reduce experimental time while running more samples.

173

174 Data availability: The .stl files for PROTeGE are available up on request.

175

176 Authors contribution: MR and DJC contributed both equally to the manuscript. The experiments were  
177 conducted by MR.

178

179 Competing interests: The authors declare that they have no conflict of interest.

180

181

182

## 183 **References**

184

185 Eerikainen, H., Watanabe, W., Kauppinen, E. I. and Ahonen, P. P: Aerosol flow reactor method for  
186 synthesis of drug nanoparticles, Euro. J. Pharma. and Biopharma., 55,3, 357-360, 2003.

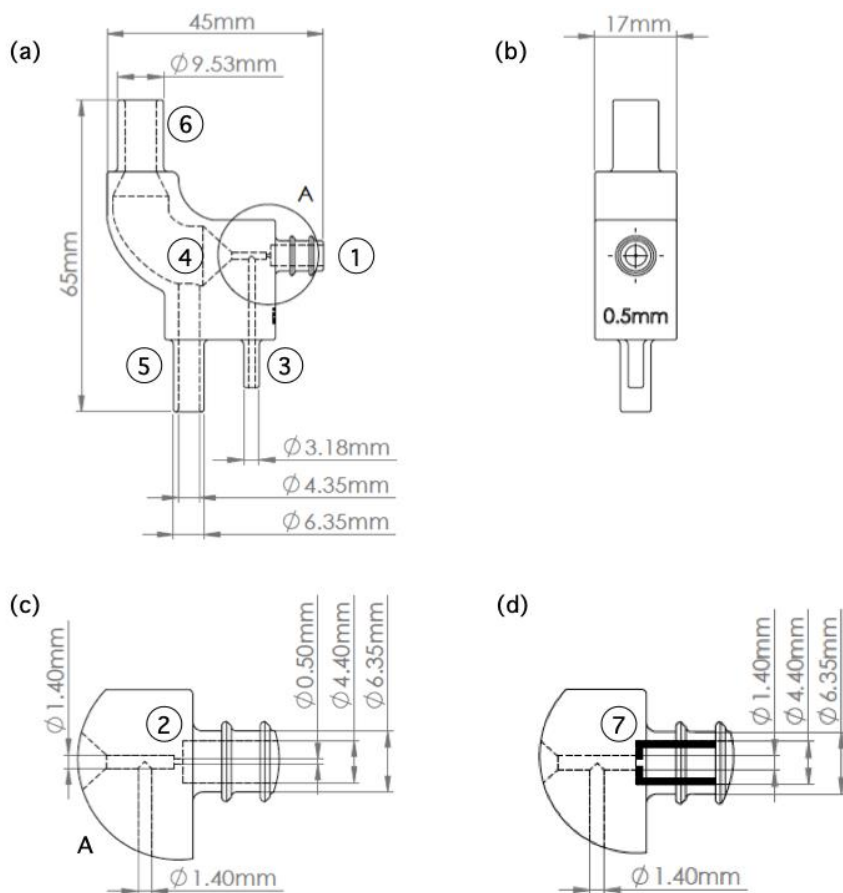
187

188 Kong, X., Wolf, M., Roesch, M., Thomson, E. S., Bartles-Rausch, T., Alpert, P. A., Ammann, M., Prisle,  
189 N. L., and Cziczo, D. J.: A continuous flow diffusion chamber study of sea salt particles acting as cloud  
190 nuclei: deliquescence and ice nucleation, Tellus B, 70, doi:10.1080/16000889.2018.1463806, 2018.



- 191
- 192 Liu, B. Y. H., and Lee, : An Aerosol Generator of High Stability, *Am. Ind. Hyg. Assoc. J.*, 36, 861–865,  
193 1975.
- 194
- 195 May, K.R.: The Collusion Nebulizer: Description, Performance and Application, *J. Aero. Sci.*, 4, 235–  
196 243, 1973.
- 197
- 198 Reisner, C., Katial, R. K., Bartelson, B. B., Buchmeir, A., Rosenwasser, L. J., Nelson, H. S.:  
199 Characterization of aerosol output from various nebulizer/compressor combinations, *A. All. Asth.*  
200 *Immun.*, 1081-1206, 86, 5, 566-574, 2001.
- 201
- 202 Roesch, M., Roesch, C., and Cziczo, D. J.: Dry particle generation with a 3-D printed fluidized bed  
203 generator, *Atmos. Meas. Tech.*, 10, 1999–2007, 2017.
- 204
- 205 Swiderska-Kowalczyk, M., Gomez, F. J., Martin, M.: Particle generation methods applied in large-scale  
206 experiments on aerosol behavior and source term studies, *Inform. Tech. Cie.*, 819, 1997.
- 207
- 208 Wex, H., Augustin-Bauditz, S., Boose, Y., Budke, C., Curtius, J., Diehl, K., Dreyer, A., Frank, F.,  
209 Hartmann, S., Hiranuma, N., Jantsch, E., Kanji, Z. A., Kiselev, A., Koop, T., Möhler, O., Niedermeier,  
210 D., Nillius, B., Rösch, M., Rose, D., Schmidt, C., Steinke, I., and Stratmann, F.: Intercomparing different  
211 devices for the investigation of ice nucleating particles using Snomax <sup>®</sup> as test substance, *Atmos. Chem.*  
212 *Phys.*, 15, 1463–1485, 2015.
- 213
- 214 Wang, J., Shilling, J. E., Liu, J., Zelenyuk, A., Bell, D. M., Petters, M. D., Thalman, R., Mei, F., Zaveri,  
215 R. and Zheng, G.: Cloud droplet activation of secondary organic aerosol is mainly controlled by molecular  
216 weight, not water solubility, *Atmos. Chem. Phys.* 19, 941-954, 2019.
- 217





218

219

220

221

222

223

**Figure 1:** Dimensioned drawings of PROTeGE: (a) side view; (b) front view; (c) detailed view of the inlet section with the printed 0.5mm orifice; (d) detailed view of the inlet section with the exchangeable nozzle/orifice. PROTeGE consists of: (1) a pressurized air inlet, (2) a printed 0.5mm orifice, (3) a liquid feed inlet, (4) a central impaction chamber, (5) the drain outlet, (6) an aerosol outlet, and an optional (7) exchangeable orifice.

224

225

226

227

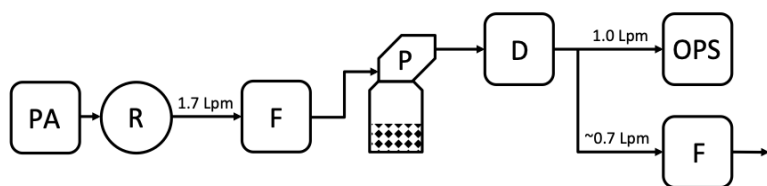
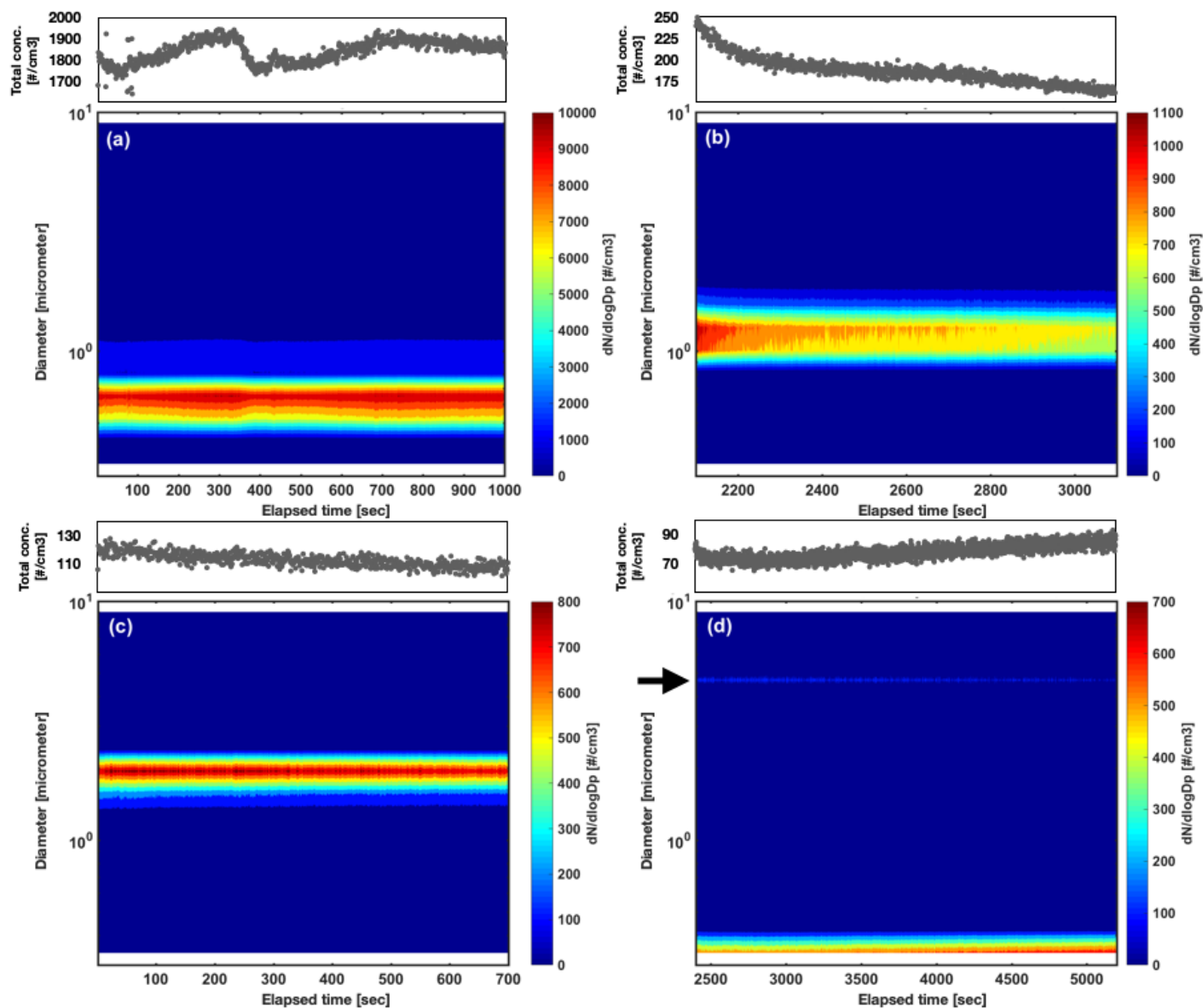


**Figure 2:** Schematic of the experimental setup used in this study. A dry pressurized air flow (PA) was passed through a rotameter (R) to control the flow rate and a filter (F) upstream of PROTeGE (P). Generated droplets were dried with silica gel (D) before the flow of particles was directed into an OPS with excess flow discarded through a filter (F).



228

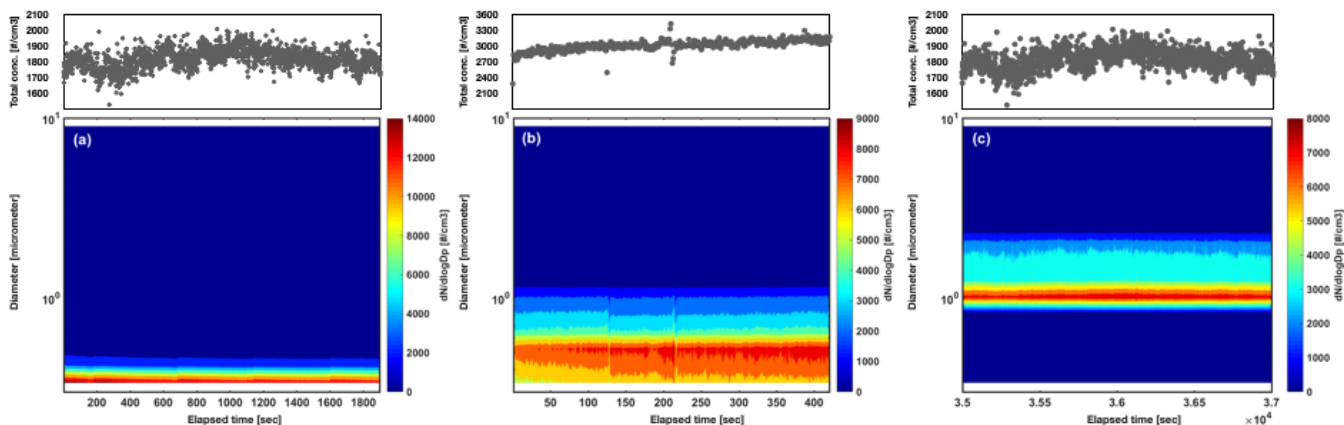


229 **Figure 3:** Total particle number concentrations and particle number size distributions as function of time for different sized polystyrene  
230 latex spheres generated with PROTeGE and detected by the OPS: (a) 0.75  $\mu\text{m}$ ; (b) 1.5  $\mu\text{m}$ ; (c) 2.0  $\mu\text{m}$ ; (d) 5.0  $\mu\text{m}$  where the black arrow  
231 denotes the PSL size and the small particles represent atomized matrix material (see text for details).

232



233

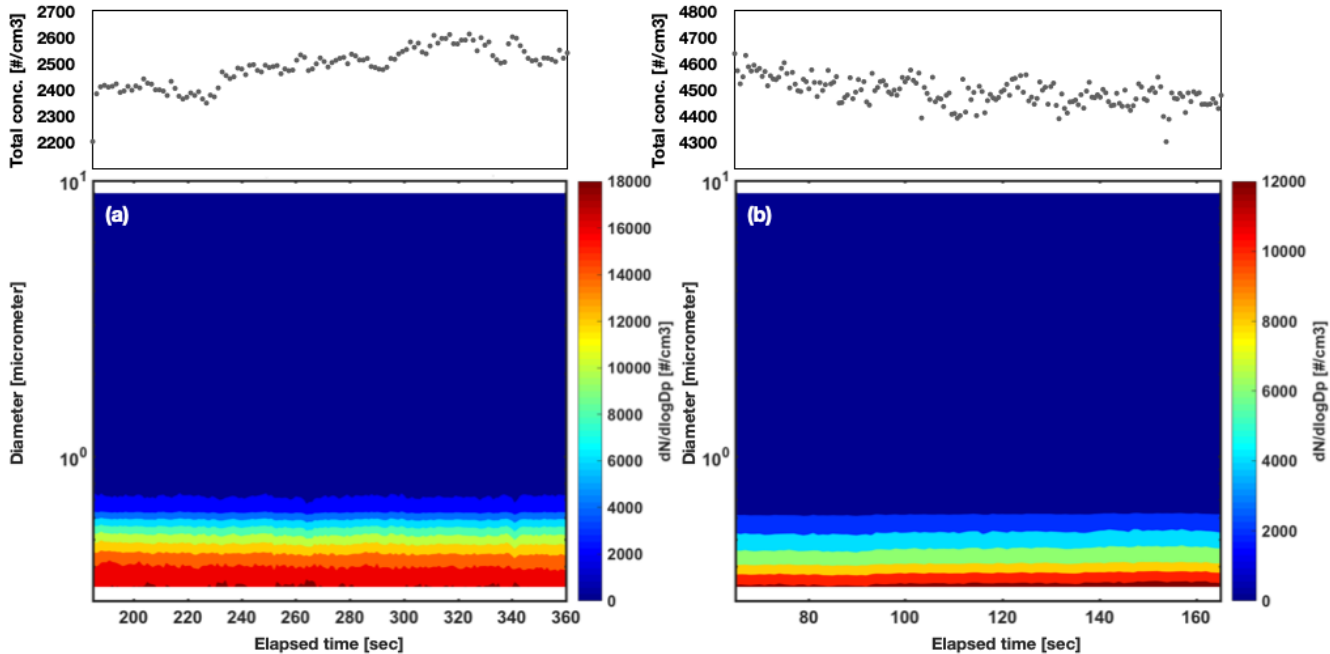


234

235

236

**Figure 4:** Total particle number concentrations and particle number size distributions as a function of time and of concentration of aqueous ammonium sulfate: (a) 0.1 g L<sup>-1</sup>; (b) 0.6 g L<sup>-1</sup>; (c) 5.0 g L<sup>-1</sup>.



237

238

239

240

**Figure 5:** Total particle number concentrations and particle number size distributions of aqueous ammonium as a function of time for sulfate particles at 0.6 g L<sup>-1</sup>: (a) 0.5mm printed orifice; (b) 0.5mm brass orifice.